Numerical studies on heat transfer and pressure drop characteristics of flat finned tube bundles with various fin materials

Y Peng[1], S J Zhang[1,3], F Shen[1], X B Wang[2], X R Yang[2] and L J Yang[2]

[1]State Power Investment Central Research Institute, South Zone of the Future Science & Technology Park, Beijing, China
[2]Key Laboratory of Condition Monitoring and Control for Power Plant Equipment of Ministry of Education, School of Energy Power and Mechanical Engineering, North China Electric Power University, No. 2 Beinong Road, Changping District, Beijing, China

E-mail: zhangshengjun@snptc.com.cn

Abstract. The air-cooled heat exchanger plays an important role in the field of industry like for example in thermal power plants. On the other hand, it can be used to remove core decay heat out of containment passively in case of a severe accident circumstance. Thus, research on the performance of fins in air-cooled heat exchangers can benefit the optimal design and operation of cooling systems in nuclear power plants. In this study, a CFD (Computational Fluid Dynamic) method is implemented to investigate the effects of inlet velocity, fin spacing and tube pitch on the flow and the heat transfer characteristics of flat fins constructed of various materials (316L stainless steel, copper-nickel alloy and aluminium). A three dimensional geometric model of flat finned tube bundles with fixed longitudinal tube pitch and transverse tube pitch is established. Results for the variation of the average convective heat transfer coefficient with respect to cooling air inlet velocity, fin spacing, tube pitch and fin material are obtained, as well as for the pressure drop of the cooling air passing through finned tube. It is shown that the increase of cooling air inlet velocity results in enhanced average convective heat transfer coefficient and decreasing pressure drop. Both fin spacing and tube pitch engender positive effects on pressure drop and have negative effects on heat transfer characteristics. Concerning the fin material, the heat transfer performance of copper-nickel alloy is superior to 316L stainless steel and inferior to aluminium.

1. Introduction

Air-cooled heat exchangers are widely used in various industries such as thermal power plants, air conditioning, refrigeration, chemical engineering, etc. The heat transfer coefficient is the dominant factor that could affect the heat transfer performance of air-cooled heat exchangers. In addition, the air-side thermal resistance of the heat exchangers is the main contributor for the total thermal resistance of the heat exchanger [1]. Generally, flat fins are arranged on the outer surface of the round tubes in order to increase the heat transfer area on the air side of heat exchangers, improve the thermal performance effectively and optimize the structure size and weight of the air-cooled heat exchanger.

There have been many studies on the heat transfer characteristics and pressure drop of the finned tubes. He *et al* [2] conducted three dimensional numerical studies on laminar flow and heat transfer of

a plate fin-and-tube heat exchanger to reveal the effects of five factors: Reynolds (Re) number, fin pitch, tube row number, spanwise and longitudinal tube pitch. It was found that the Nusselt number increased with the increase of Re number an optimum fin pitch at which the Nusselt number became maximum existed, and the increase of the number of tube rows led to decrease of the average Nusselt number. Kang *et al* [3] carried out a systematic experimental investigation on heat transfer and pressure drop characteristics of four types of plate fin-and-tube heat exchanger surfaces: the plain plate, the slotted plain, the wavy fin with triangular cross section and the wavy fin with sinusoidal cross section. They found that the Nusselt number of the slotted plain fin surface and of the plain plate fin were the greatest and the lowest respectively, while the thermal performance of those two with the wavy fins was between them. Three-dimensional simulations were made to investigate heat transfer and fluid flow characteristics of a four row plain fin-and-tube heat exchanger considering in-lined and staggered arrangements by means of the CFD commercial software ANSYS CFX [4], which revealed the effects of Reynolds number, fin pitch and tube pitch on the overall heat transfer and friction factor for plate fin-and-tube heat exchangers.

On the other hand, air-cooled heat exchangers could also be utilized in nuclear power plants to remove the core decay of residual heat from inside of the containment under severe accident circumstances. Component standards in nuclear power field differ from the ones in traditional industries (such as conventional thermal power plants), especially in issues concerning materials. In terms of environmental conditions in nuclear power plants, like irradiation and corrosion, it is necessary to pay attention to material selection for the fins and tubes of air-cooled exchangers. With respect to these conditions, three kinds of materials, namely 316L stainless steel, copper-nickel alloy and aluminium, are selected as candidates. Copper for example plays the important role in the material choice due to its favorable corrosion resistance, ductility, electric and thermal conductivity. However, its expensive price is the main restrictive factor, so seeking alternative materials is the trend in current research. Li [5] carried out a numerical simulation method to study the heat transfer coefficient of different materials of finned tube bundles in dry conditions, on the basis of the same boundary condition. As a result, the required quantity and cost of different heat exchanger materials were obtained, as well as the theory basis for material replacement of finned tube bundles was provided. For the material selection of finned tube bundles, the price of aluminium is much less than the copper, so comparison of the performance of these two materials is essential, Chen [6] analyzed the variations of heat transfer coefficient and heat transfer rate and it had proved that it is feasible to replace the copper with aluminium. In addition, environmental conditions and especially the blowing wind is also a basic factor for the heat transfer characteristics of finned tube bundles. For such and air-cooled condenser of a power plant, Yang [7] established the physical and mathematical models for the fluid and heat flow characteristics and obtained various results for the flow resistance and average convection heat transfer coefficient with different windward velocities. Hu *et al* [8] presented a new and reliable model to predict the flow and heat transfer characteristics of an air-cooled condenser under the influence of natural wind based on POD (Proper Orthogonal Decomposition) methods in order to account for the three-dimensional velocity and temperature fields when the natural wind directions ranging from 0 to 90 degrees. The heat transfer characteristics of stainless steel at different wind velocities were analyzed by Shi [9]; the results showed that increasing inlet velocity appropriately can improve the heat transfer performance of the finned tube bundles. Kong *et al* [10] performed a three-dimensional numerical study on the variations of friction factor, heat flow rate and convection heat transfer coefficient of flat and slotted finned tube bundles under various wind velocities, which indicated that heat flow rate and convection heat transfer coefficient raised continuously, while the friction factor decreased with the lower wind speed.

The studies mentioned above are few and there is still the need for further studies on the finned tube materials in conjunction with different wind speed at home and abroad. In the present study, the heat transfer performance of fins and tubes, constructed of three different materials (copper-nickel alloy, 316L stainless steel, and aluminium) and for different wind velocities are investigated, in order to benefit for the design of air-cooled exchangers in nuclear power plants. To this end, several

simulations in order to numerically predict the heat transfer characteristics and pressure drop of fin-and-tube heat exchangers for different materials and various inlet velocities are carried out.

2. Models

2.1. Physical model and boundary conditions

Figure 1 shows the schematic diagram of the flat fin-and-tube bundles, which are arranged in a staggered pattern. In doing so, the existence of fins and the tube arrangement can greatly the heat transfer surface area and enhance the flow disturbance, contributing to the enhancement of heat transfer performance of air-cooled heat exchangers.

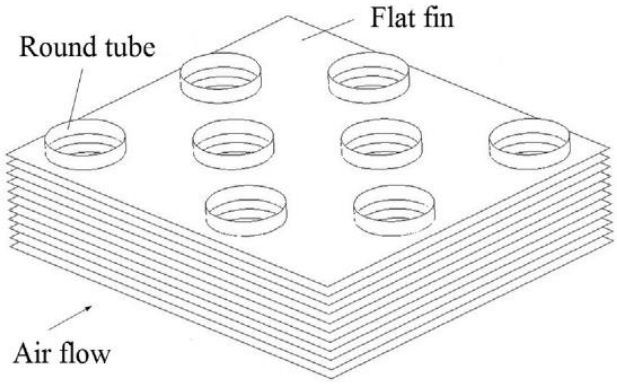

Figure 1. Schematic diagram of flat finned tube bundles [10].

The schematic diagram and geometric details of the flat finned tube bundles used in this study are described in figure 2, while. The corresponding dimensions are listed in table 1.

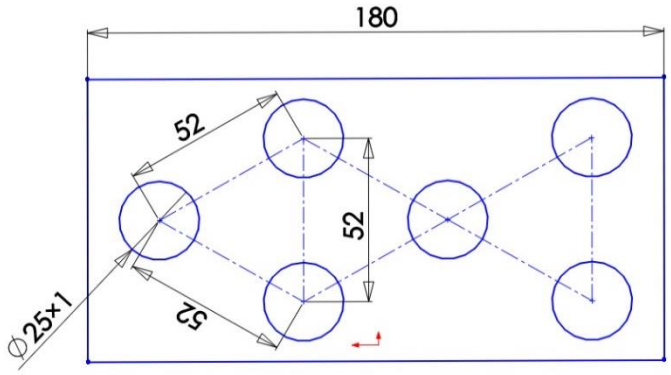

Figure 2. Schematic diagram of the tube arrangement.

Table 1. Dimensions of the flat finned tubes.

Parameter	Value
Base tube (outer diameter and thickness)/mm×mm	Φ25×1
Fin (width and thickness)/ mm×mm	180×0.12
Fin-pitch/mm	2.4, 2.8, 3.2, 3.6, 4.0
Tube row number	4
Tube pitch/mm	34, 40, 46, 52

Figure 3 shows the main computational domain for the flat fin-and-tube configuration and its boundaries, in which inlet, outlet, symmetry, wall and periodic boundary conditions are applied at the corresponding parts of the boundary. In order to ensure uniform air flow at the inlet and avoid backflow at the outlet that could pose negative effects on computational convergence, extended areas are added in the computational domain, as is depicted in figure 4. The inlet and outlet part extends 270 mm and 900 mm in the X-direction of the computational domain, respectively, so that uniform inlet velocity distribution could be applied to the inlet as well as the fully-developed outflow boundary to the outlet. A velocity inlet boundary condition was implemented at the inlet of the computational domain with inlet velocity ranging from 0.25 m/s to 2 m/s and constant air inlet temperature 323.15 K. No-slip conditions for momentum and constant temperature 363.15 K are set for the inner surfaces of the base tube while at its outer surfaces coupled thermal conditions are imposed. Hence, the temperature distribution both on the solid surface and the fluid side can be calculated simultaneously with the flow field by solving the conjugate problem. In addition, the Z-direction is periodic and the Y-direction is symmetry boundary condition.

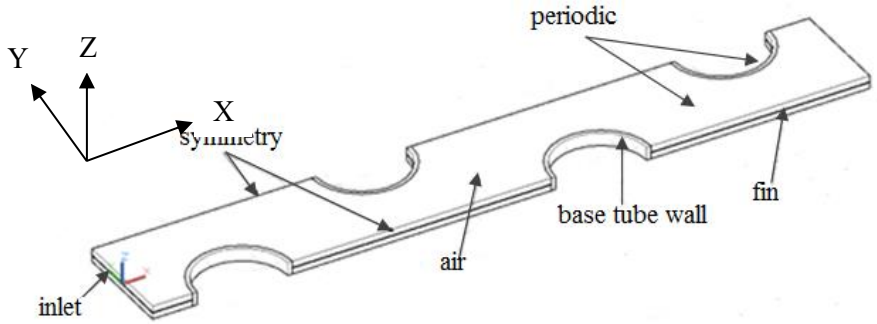

Figure 3. Boundary conditions for finned tube bundles.

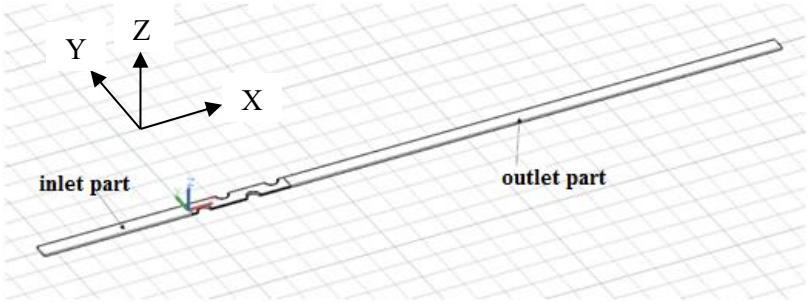

Figure 4. Extended domains for finned tube bundles.

The computational mesh was created by the commercial software GAMBIT. For the inlet and outlet part, hexahedral structured mesh was adopted since they are regular hexagons, as shown in figure 5. In the fin-and-tube region, the relative coarse hexahedral unstructured grids were generated for the flow channel, and the mesh near the walls was refined to capture flow and heat transfer details accurately around the tube. The schematic mesh around the tube-and-fin is presented in figure 6.

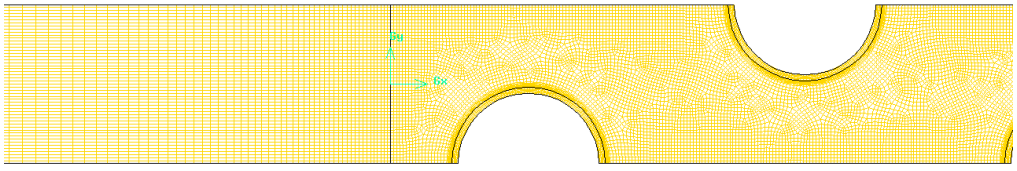

Figure 5. Schematic mesh for the input part.

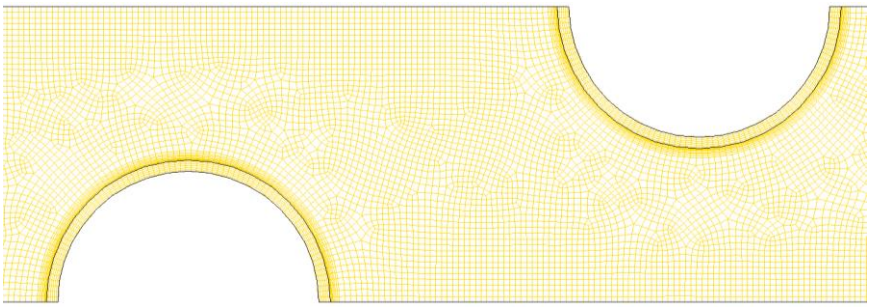

Figure 6. Schematic mesh around the fin-and-tube domains.

2.2. Governing equations

Numerical studies are conducted based on the assumptions that the fluid is incompressible, its physical properties are constant, and the flow is steady-state turbulent. The governing equations including continuity, momentum and energy equations for the computational domain can be expressed in tensor form as follows.

Continuity equation:

$$\frac{\partial \rho u_i}{\partial x_i} = 0 \tag{1}$$

Momentum equation:

$$\frac{\partial}{\partial x_i}(\rho u_i u_j) = -\frac{\partial p}{\partial x_i} + \frac{\partial \tau_{ij}}{\partial x_j} + \frac{\partial}{\partial (x_j)}\left(-\rho \overline{u_i' u_j'}\right) \tag{2}$$

where

$$\tau_{ij} = \mu\left(\frac{\partial u_i}{\partial x_j} + \frac{\partial u_j}{\partial x_i} - \frac{2}{3}\delta_{ij}\frac{\partial u_k}{\partial x_k}\right) \tag{3}$$

According to Boussinesq hypothesis, the turbulent shear stress can be written as the following form in which the Reynolds stress is analogous to the shear stress of laminar flow.

$$-\rho \overline{u_i' u_j'} = \mu_t\left(\frac{\partial u_i}{\partial x_j} + \frac{\partial u_j}{\partial x_i} - \frac{2}{3}\delta_{ij}\frac{\partial u_k}{\partial x_k}\right) - \frac{2}{3}\delta_{ij}\rho k \tag{4}$$

Energy equation:

$$\frac{\partial}{\partial x_i}(\rho u_i H) = \frac{\partial}{\partial x_i}\left(\lambda \frac{\partial T}{\partial x_i} + \frac{\mu_t}{\sigma_t}\frac{\partial H}{\partial x_i}\right) + u_i \frac{\partial P}{\partial x_i} + S_h \tag{5}$$

Turbulence kinetic energy equation:

$$\frac{\partial}{\partial x_i}(\rho k u_i) = \frac{\partial}{\partial x_j}\left(\left(\mu + \frac{\mu_t}{\sigma_k}\right)\frac{\partial k}{\partial x_j}\right) + G_k + G_b - \rho\varepsilon - Y_M + S_k \tag{6}$$

Turbulence dissipation rate equation:

$$\frac{\partial}{\partial x_i}(\rho \varepsilon u_i) = \frac{\partial}{\partial x_j}\left(\left(\mu + \frac{\mu_t}{\sigma_\varepsilon}\right)\frac{\partial \varepsilon}{\partial x_j}\right) + C_{1\varepsilon}\frac{\varepsilon}{k}(G_k + C_{3\varepsilon}G_b) - C_{2\varepsilon}\rho\frac{\varepsilon^2}{k} + S_\varepsilon \tag{7}$$

In these equations, G_k represents the generation of turbulence kinetic energy due to mean velocity gradients, $G_b$represents the generation of turbulence kinetic energy due to buoyancy, Y_M represents the contribution of the fluctuating dilatation in compressible turbulence to the overall dissipation rate, $C_{1\varepsilon}$, $C_{2\varepsilon}$, and $C_{3\varepsilon}$ are constants, σ_k and σ_ε are the turbulent Prandtl numbers for k and ε respectively and S_k and S_ε are the source terms.

2.3. Numerical method

The governing equations mentioned above are solved by the commercial CFD software Fluent 16 [11] with the finite volume method. The continuity, momentum and energy equations are used second-order upwind spatial discretization scheme, and the SIMPLE algorithm is applied to the pressure-velocity coupling iterative computation. The convergence criterion for residual values of governing equations was set to 10^{-6}.

2.4. Parameter definition

For the flow and heat transfer characteristics calculation, the following parameters defined below in order to improve the understanding on post processing of the results.

$$h = \frac{\emptyset}{A \cdot \Delta T_m} \tag{8}$$

$$\Delta T_m = \frac{T_o - T_{in}}{ln\left(\frac{T_w - T_{in}}{T_w - T_o}\right)} \tag{9}$$

$$\emptyset = c_p m_a (T_o - T_i) \tag{10}$$

$$\Delta P = P_{in} - P_{out} \tag{11}$$

$$KL = \frac{\Delta P}{\frac{1}{2}\rho u^2} \tag{12}$$

where T_o and T_{in} are the area-weighted average temperatures at the outlet and inlet surfaces respectively, T_w is the fluid-side wall temperature, m_a is the air mass flow rate, P_{in} and P_{out} represent the inlet and outlet pressures respectively and KL is the friction factor.

3. Results and discussion

3.1. Effects of inlet velocity and material

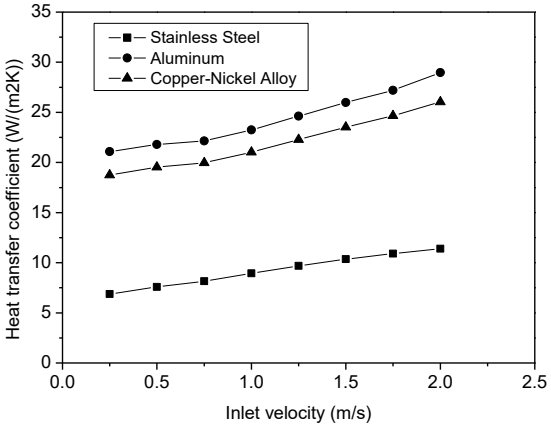

Figure 7. The effects of inlet velocity on heat transfer coefficient for different fin and tube materials.

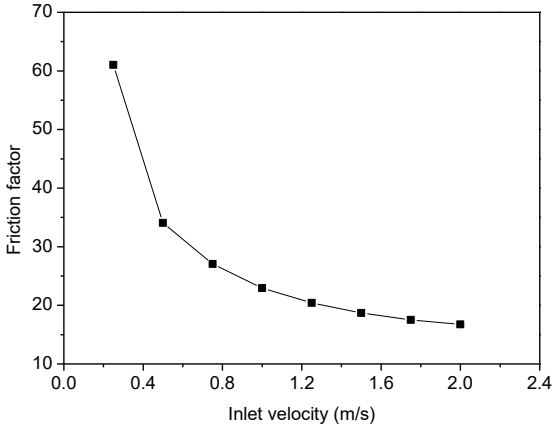

Figure 8. The effects of inlet velocity on friction factor.

The effects of the air velocity on heat transfer characteristics with constant fin spacing 3.2 mm and tube pitch 52 mm are investigated for the following values of inlet velocity: 0.25 m/s, 0.5 m/s, 0.75 m/s, 1 m/s, 1.25 m/s, 1.5 m/s, 1.75 m/s and 2 m/s. Figure 7 shows the numerical results obtained for stainless steel, aluminium and copper-nickel alloy fin-and-tubes with different inlet air velocity. The heat transfer coefficient increases with the increase of inlet velocity. The maximum values for stainless

steel, aluminium and copper-nickel alloy in this speed condition are approximately 11.34, 28.87 and 24.57 W/(m^2·K) respectively, while the corresponding minimum values are 6.88, 21.08 and 18.74 W/(m^2·K). It can be seen clearly that the aluminium is the most effective material on heat transfer, and the copper-nickel alloy works better than the stainless steel. In particular, the heat transfer coefficient of aluminium is about 60.7% higher than that of stainless steel at the same inlet velocity.

The pressure drop characteristics are independent of the fin-and-tube material according to the results of friction factor calculations for three kinds of materials. Since the friction factor for different materials is almost identical, only the friction factor of stain steel is presented in figure 8. The friction factor decreases sharply under the value of 1 m/s inlet velocity, and then declines gradually when the inlet velocity is higher than 1 m/s. It is can be concluded that the inlet velocity has a great impact on pressure drop characteristics.

3.2. Effects of fin spacing and material

Figure 9 compares the heat transfer coefficient of flat finned tube bundles for the various different materials of construction for fin spacing ranging from 2.4 mm to 4.0 mm and inlet velocity 0.5 m/s. The heat transfer coefficient decreases with the increase of fin spacing. The maximum values of the heat transfer coefficient are 7.998, 27.470 and 23.853 W/(m^2·K) for stainless steel, aluminium and copper-nickel alloy, respectively. The results also show that the heat transfer coefficient of aluminium is 243% higher than that of stainless steel at the same inlet velocity and fin spacing.

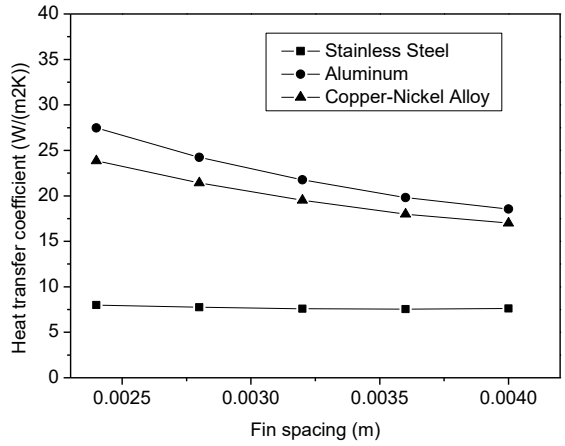

Figure 9. The effects of fin spacing on heat transfer coefficient (inlet velocity 0.5 m/s, tube pitch 52 mm).

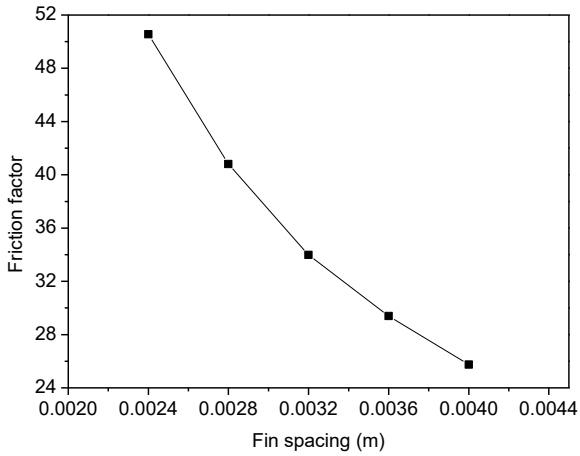

Figure 10. The effects of fin spacing on friction factor (inlet velocity 0.5 m/s, tube pitch 52 mm).

Since the simulated pressure drop coefficient corresponding to the three different materials are closely identical, only one friction factor curve is presented. The effects of fin spacing at the constant velocity on friction factor are depicted in figure 10. The friction factor decreases steeply when the fin spacing is increasing. It is shown that the increase of fin spacing contributes clearly to the reduction of the friction coefficient and the pressure drop (since the velocity is constant).

3.3. Effects of Tube pitch and material

The variation of the heat transfer coefficient for the three different materials as the tube pitch ranges from 34 mm to 52 mm with constant inlet velocity 1.0 m/s is depicted in figure 11. Along with the increase of tube pitch, the heat transfer coefficient decreases gradually. The thermal performance of copper-nickel is better than that of stainless steel, but inferior to that of aluminium. Figure 11 shows that the heat transfer coefficient of aluminium is 67% higher than that of stainless steel at the same inlet velocity and fin spacing.

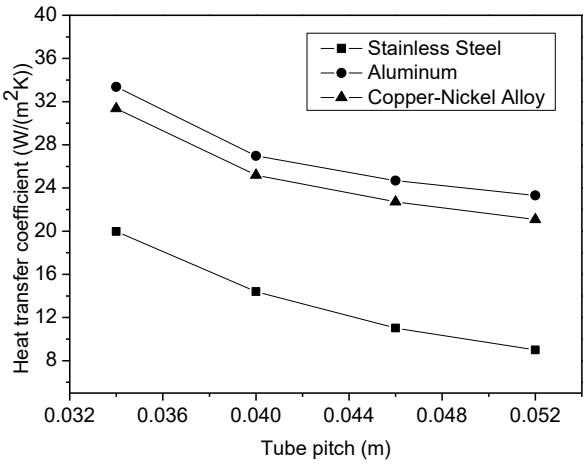

Figure 11. The effects of tube pitch on heat transfer coefficient (inlet velocity 1 m/s, fin spacing 3.2 mm).

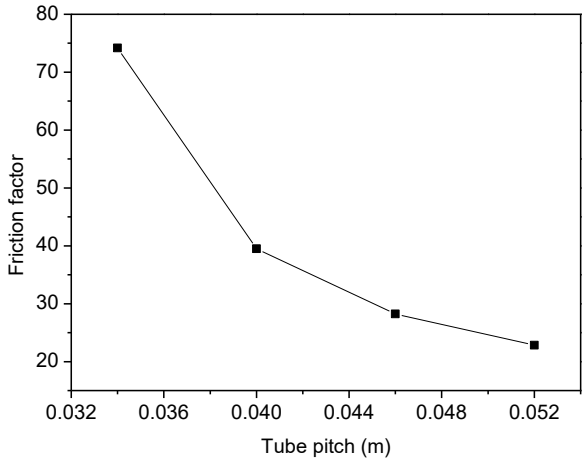

Figure 12. The effects of tube pitch on friction factor (inlet velocity 1 m/s, fin spacing 3.2 mm).

As before, the friction factor is given only for one type of material. Figure 12 shows the effects of tube pitch on friction factor. The friction factor decreases steeply when the tube pitch is ranging from 34 mm to 40 mm and drops gently afterwards. The result shows that the increase of tube pitch leads to reduction of the pressure drop.

4. Conclusions

The heat transfer and pressure drop characteristics for different fin-and-tube materials at various inlet velocities, fin spacing and tube pitches were numerically investigated. To this end, the flow and temperature fields were numerically simulated and the heat transfer coefficient and the friction factor were numerically predicted. The most effective material for heat transfer was proved to be aluminium, the heat transfer coefficient of which is much higher than that of stainless steel. Between the other two materials tested, copper-nickel alloy works better than the stainless steel in terms of the heat transfer coefficient. The heat transfer coefficient increases with the increase of inlet velocity, and decreases with the increase of fin spacing as well as the tube pitch for all the materials. The friction factors are almost identical for all the materials, i.e. pressure drop is independent of the fin-and-tube material. The friction factor has a clear decrease when the inlet velocity, fin spacing, and tube pitch increase. The heat transfer coefficient and pressure drop variation with various materials at different inlet velocity, fin spacing and tube pitch is expected to provide the useful information for reference in fin-and-tube material selection in engineering application.

Nomenclature

Nomenclature		Greek symbols	
A	area (m^2)	μ_t	turbulent viscosity (kg/(m·K))
x,y,z	coordinates (m)	μ	dynamic viscosity (Pa s)
u	velocity (m/s)	τ	shear stress (Pa)
P	pressure (Pa)	ρ	density (kg/m^3)
H	enthalpy (J/kg)	ε	Kinetic energy dissipation rate
S	source term	k	turbulent kinetic energy (m^2/s^2)
T	temperature (K)	λ	thermal conductivity (W/(m K))
h	heat transfer coefficient ($W/(m^2 \cdot K)$)	in	inlet
ΔT_m	logarithmic mean temperature difference (K)	O	outlet
ΔP	pressure drop (Pa)	σ	turbulent Prandtl number
c_p	specific heat at constant pressure (J/(kg·K))	Φ	heat flow rate (W)

m_a	air flow mass rate (kg/s)
KL	friction factor

Acknowledgments
This work is supported by the National Key Science and Technology Project (2015ZX06004004).

References
[1] Wang C-C, Chang Y-J, Hsieh Y-C and Lin Y-T 1996 Sensible heat and friction characteristics of plate fin-and-tube heat exchangers having plane fins *Int J Refrig* **19** 223-30
[2] He Y L, Tao W Q, Song F Q and Zhang W 2005 Three-dimensional numerical study of heat transfer characteristics of plain plate fin-and-tube heat exchangers from view point of field synergy principle *Int J Heat Fluid Fl* **26** 459-73
[3] Kang H J, Li W, Li H Z, Xin R C and Tao W Q 1994 Experimental study on heat transfer and pressure drop characteristics of four types of plate fin-and-tube heat exchanger surfaces *J Therm Sci* **3** 34-42
[4] Bhuiyan A A, Amin M R and Islam A K M S 2013 Three-dimensional performance analysis of plain fin tube heat exchangers in transitional regime *Appl Therm Eng* **50** 445-54
[5] Li J 2014 Numrical simulation study of finned tube heat exchanger performance with different materials (Guangzhou: Guangzhou University)
[6] Li C 2008 Analysis about aluminum replaced of copper in heat exchanger manufacture The 13th Academic Conference of Heat Pump and Systematic Energy-saving Technology (Gansu, China) p 4
[7] Yang L J, Jia S N, Bi Y D, Du X Z and Yang Y P 2012 Numerical study on flow and heat transfer characteristics of finned tube bundles for air-cooled heat exchangers of indirect dry cooling systems in power plants *Proceedings of the Chinese Society for Electrical Engineering* 50-8
[8] Hu H, Du X, Yang L and Yang Y 2014 POD based modeling on flow and heat transfer of air-cooled condenser influenced by natural wind *Int J Heat Mass Tran* **74** 431-40
[9] S. Xinwu, 2012 The analysis of flow resistance and heat transfer characteristics of the stainless steel fin tube heat exchanger (Guangzhou: South China University of Technology)
[10] Kong Y Q, Yang L J, Du X Z and Yang Y P 2016 Air-side flow and heat transfer characteristics of flat and slotted finned tube bundles with various tube pitches *Int J Heat Mass Tran* **99** 357-71
[11] Fluent A 2011 *Ansys Fluent Theory Guide* (ANSYS Inc., USA) **15317** 724-46